Journal of ELECTRICAL ENGINEERING, VOL. 59, NO. 5, 2008, 225–233

NEW ANTI–SKID CONTROL FOR ELECTRIC VEHICLE USING BEHAVIOUR MODEL CONTROL BASED ON ENERGETIC MACROSCOPIC REPRESENTATION

Kada Hartani [*] — **Mohamed Bourahla** [**] — **Yahia Miloud** [*]

The contribution of each wheel to the advance of the vehicle is represented by a mechanical coupling of accumulation element. However, by taking into account the contact wheel-road, a new problem occurs which can be associated with the mechanical coupling, adding to that, the principle of contact which is badly known, nonlinear and non-stationary. The whole of these phenomena (mechanical coupling and skid) will induce different resistive torques for the machines. The problems arising from the mechanical coupling are related to the nonlinear character of the contact wheel-road. The solution of this problem is obtained by using a model control structure adapted well to the nonlinear systems: the behaviour model control (BMC). A specific formalism based on energetic conversion is used to model an electric vehicle using two permanent magnet synchronous motors. From this modelling, a complete model of the electromechanical system is implemented in simulation which includes both PMS motors, the wheels and vehicle dynamics induced by the adhesion phenomenon. The simulations carried out using Matlab/Simulink showed that the non linear problem of adhesion is solved by the behaviour model control in which the skid phenomenon has completely disappeared and the stability of vehicle is assured.

K e y w o r d s: behaviour model control; anti-skid control; multi-machine control; electric vehicle

1 INTRODUCTION

In this paper, two permanent magnet synchronous motors which are supplied by two voltage inverters are used. The system of traction studied Fig. 1, belongs to the category of the multi-machines multi-converters systems (MMS). The number of systems using several electrical machines and/or static converters is increasing in electromechanical applications. These systems are called multi-machines multi-converters systems [1]. In such systems, common physical devices are shared between the different energetic conversion components. This induces couplings (electrical, mechanical or magnetic) which are quite difficult to solve [2]. The complexity of such systems requires a synthetic representation in which classical modelling tools cannot always be obtained. Then, a specific formalism for electromechanical system is presented based on a causal representation of the energetic exchanges between the different conversion structures which is called Energetic macroscopic representation (EMR). The studied MMS is an electric vehicle. This system has a mechanical coupling Fig. 1. The main problem of the mechanical coupling is induced by the non-linear wheel-road adhesion characteristic. A specific control structure well adapted to the non-linear system (the Behaviour Model Control) is used to overcome this problem. The BMC has been applied to a non-linear process, however the wheel-road contact law of a traction system can be solved by a linear model. The control of the traction effort transmitted by each wheel is at the base of the command strategies aiming on improving the stability of a vehicle. Each wheel is controlled independently by using an electric motorization. However, the traditional thermal motorization always requires the use of a mechanical differential to ensure the distribution of power on each wheel. The mechanical differential usually imposes a balanced transmitted torques. For an electric traction system, this balance can be obtained by using a multi-motor structure which is shown in Fig. 1. An identical torque on each motor is imposed using a classical method. The difficulty of controlling such a system is its highly nonlinear character of the traction forces expressions. The loss of adherence of one of the two wheels which is likely to destabilize the vehicle needs to be solved in this paper.

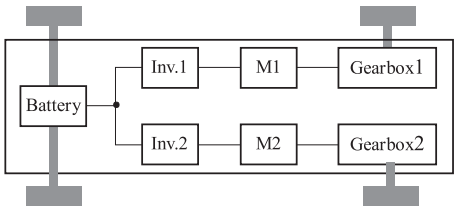

Fig. 1. Configuration of the traction system proposed

2 PRESENTATION OF THE TRACTION SYSTEM

The proposed traction system is an electric vehicle with two drives, Fig. 1. Two machines thus replace the standard case with a single machine and a differential mechanical. The power structure in this paper is composed of two permanent magnet synchronous motors which are

[*] University center of Saida, BP 138 En-Nasr, 20000 Saida, Algeria; kada_hartani@yahoo.fr [**] University of Sciences and Technology of Oran, BP 1505, El Mnaouar, 31000 Oran, Algeria

ISSN 1335-3632 © 2008 FEI STU

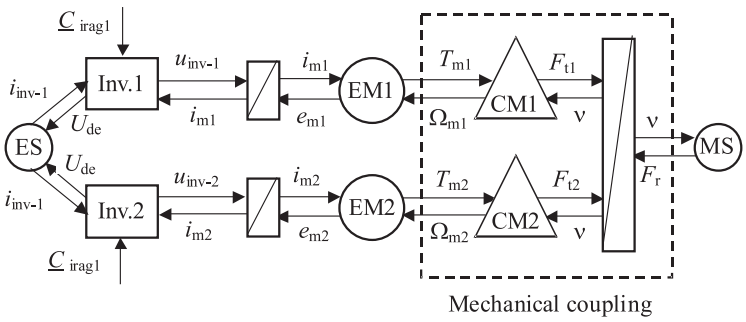

Fig. 2. EMR of the studied traction chain

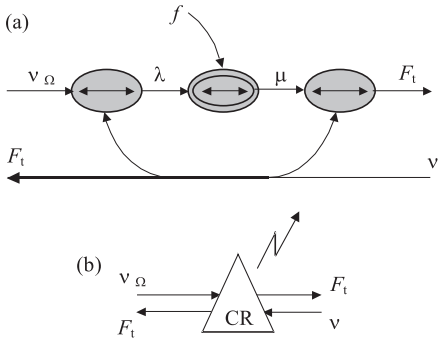

Fig. 4. Modelling of the contact wheel-road: (a) COG and (b) EMR

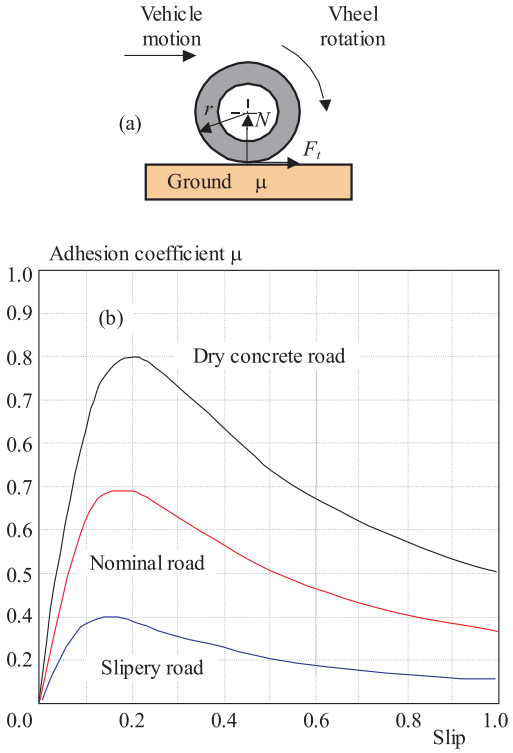

Fig. 3. (a) Forces applied to the wheel, (b) contact wheel-road characteristics.

supplied by two three-phase inverters and driving the two rear wheels of a vehicle trough gearboxes, Fig. 1. The objective of the structure is to reproduce at least the behaviour of a mechanical differential by adding to it a safety anti-skid function.

2.1 Energetic macroscopic representation of the traction system

The energetic macroscopic representation is a synthetic graphical tool on the principle of the action and the reaction between elements connected [3, 4]. The energetic macroscopic representation of the traction system proposed, Fig. 2, revealed the existence of only one coupling called overhead mechanical type which is on the mechanical part of the traction chain.

The energetic macroscopic representation of the mechanical part of the electric vehicle (EV) does not take into account the stated phenomenon. However, a fine modelling of the contact wheel-road is necessary and will be detailed in the following sections.

2.2 Mechanical transmission modelling of an electric vehicle

2.2.1 Modelling of the contact wheel-road

The traction force between the wheel and the road, Fig. 3.(a), is given by

$$F_t = \mu N \tag{1}$$

where N is the vertical force and μ the adhesion coefficient. This coefficient depends on several factors, particularly on the slip λ and the contact wheel-road characteristics [5, 6]. We define the slip λ in the acceleration mode by [7]:

$$\lambda = \frac{v_\Omega - v}{v_\Omega}\,. \tag{2}$$

The wheel speed can be expressed as

$$v_\Omega = r\Omega \tag{3}$$

where Ω is the angular speed of the wheel, r is the wheel radius and v is the vehicle speed.

Principal non-linearity affecting the vehicle stability is the adhesion function which is given by Eq. (4) and represented on Fig. 3.(b).

$$\mu = f(\lambda)\,. \tag{4}$$

The adhesion coefficient μ, which is the ratio between the wheel traction force and the normal road, depends on the wheel road conditions and the values of the wheel slip λ. In our simulations, the function $\mu(\lambda) = \left(2\mu_p\lambda_p\lambda/\lambda_p^2+\lambda^2\right)$ is used for a nominal curve, where mu_p and λ_p are the peak values. For various road conditions, Fig. 3.(b). the curves have different peak values and slopes. The adhesion coefficient-wheel slip characteristics are also influenced by operational parameters like speed and vertical load.

We now represent in the form of a COG [8] and an EMR, the mechanical conversion induced by the contact wheel-road, Fig. 4.

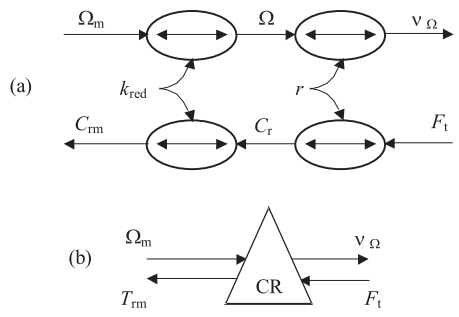

Fig. 5. Modelling of the mechanical drive: (a) COG and (b) EMR

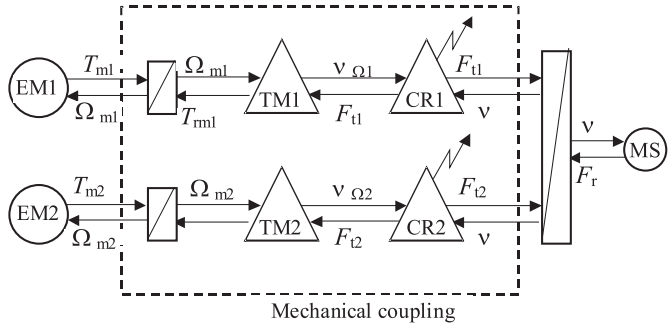

Fig. 6. Detailed EMR of the mechanical coupling

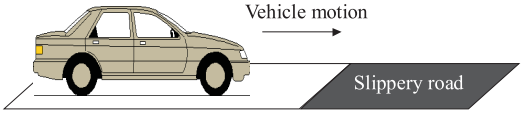

Fig. 7. The sudden road condition change

2.2.2. Modelling of the transmission gearbox-wheel

Modelling of the transmission gearbox-wheel is carried out in a classical way which is given by:

$$\begin{aligned} v_\Omega &= r\Omega\,, \\ T_r &= rF_t\,, \end{aligned} \tag{5}$$

$$\begin{aligned} \Omega &= k_{red}\Omega_m\,, \\ T_{rm} &= k_{red}T_m\,, \end{aligned} \tag{6}$$

where r is the wheel radius, k_{red} the gearbox ratio, T_r the transferred resistive torque on the wheel shafts and T_m the transferred resistive torque on the motor axle shafts, Fig. 5.

2.2.3 Modelling of the environment

The external environment is represented by a mechanical source (MS) on Fig. 2, leading to the resistance force of the vehicle motion F_r [9, 10], where:

$$F_r = F_{aero} + F_{roll} + F_{slope}\,. \tag{7}$$

F_{roll} is the rolling resistance, F_{aero} is the aerodynamic drag force and F_{slope} is the slope resistance.

The rolling resistance is obtained by Eq. (8), where μ is the rolling resistance coefficient, M is the vehicle mass and g is the gravitational acceleration constant.

$$F_{roll} = \mu Mg\,. \tag{8}$$

The resistance of the air acting upon the vehicle is the aerodynamic drag, which is given by Eq. (9), where ρ is the air density, C_D is the aerodynamic drag coefficient, A_f is the vehicle frontal area and V_h is the vehicle speed [11].

$$F_{aero} = \frac{1}{2}\rho C_D A_f V_h^2\,. \tag{9}$$

The slope resistance and down grade is given by Eq. (10)

$$F_{slope} = Mgp_{\%}\,. \tag{10}$$

When the vehicle is climbing up, the sign is positive, when the vehicle is down, the sign is negative.

2.3 EMR of the mechanical coupling

The modelling of the phenomenon related to the contact wheel-road enables us to separate the energy accumulators of the process from the contact wheel-road. However, the energy accumulators which are given by the inertia moments of the elements in rotation can be represented by the total inertia moments of each shaft motor J_Ω and the vehicle mass M, where:

$$J_\Omega \frac{\mathrm{d}\Omega_m}{\mathrm{d}t} = T_m - T_{rm} - f\Omega_m \tag{11}$$

and

$$M\frac{\mathrm{d}v}{\mathrm{d}t} = F_{t1} + F_{t2} - F_r\,, \tag{12}$$

F_{t1}, F_{t2} are the traction forces developed by the left and right wheels and F_r is the resistance force of the motion of the vehicle.

The final modelling of the mechanical transmission is represented by the EMR, Fig. 6.

2.4. The skid phenomenon

The skid phenomenon is simulated by utilizing the EV system as shown in Fig. 7. The control method used in this paper for the motors is the direct torque control (DTC) which will give to the vehicle a dynamic behaviour similar to that imposed by a mechanical differential [12–14]. However, the test consists, under these conditions, to simulate the passage of wheel 1 of the electric vehicle from a dry road to a slippery road (at $t = 6$ s) by maintaining a constant torque on each wheel ($T_{m\_ref} = 50$ Nm). The parameters of the vehicle model are given in Table 1.

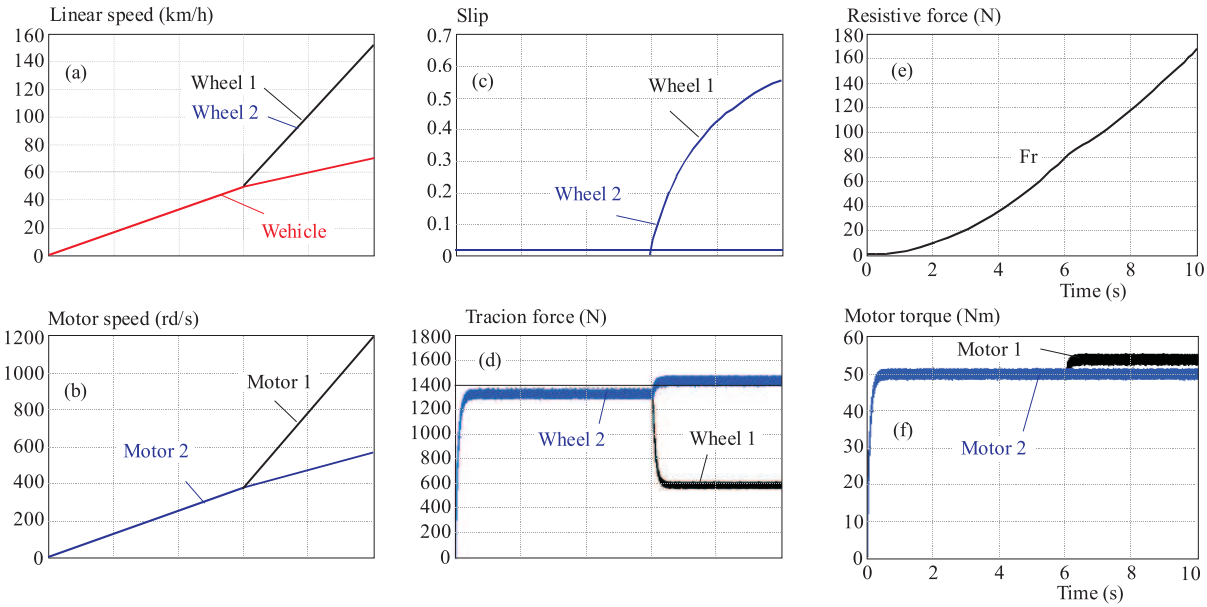

Fig. 8. Simulation results of the skid phenomenon.

From the moment of disturbance, the speed of the disturbed wheel (wheel 1) deviates from that of the vehicle, Fig. 8(a) [15–17]. The slip increases highly which causes a skid phenomenon, Fig. 8(c). This phenomenon will lead to the instability of the vehicle for two reasons:

- The imbalance of the traction forces, Fig. 8(d).
- A reduction in the side forces necessary to maintain the vehicle on its trajectory [18].

3 CONTROL STRATEGY

3.1 Maximum control structure

The maximum control structure is obtained systematically by applying the principles of inversion to the model EMR of the process [19]. We define by this method the control structure relating to the mechanical model of the vehicle. In our application, the variable to be controlled is the vehicle speed by acting on the motor torques of both wheels. The maximum control structure is shown in Fig. 9, by taking into account only one wheel for simplification.

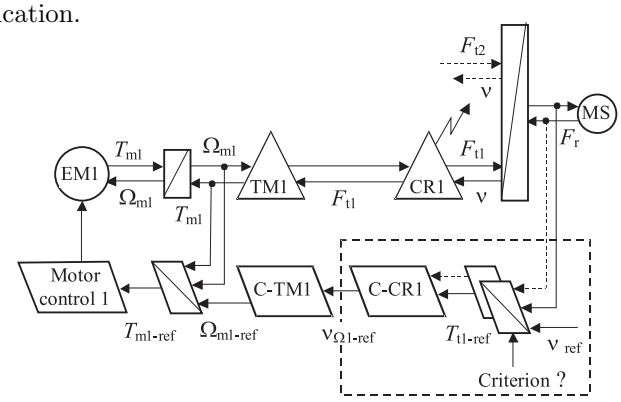

Fig. 9. EMR of the maximum control of the vehicle.

This structure shows the problems involved in the inversions of the mechanical coupling by the accumulation element and of non-linearity relating to the contact wheel-road.

3.1.1 Inversion of the coupling by accumulation elements

The inversion of the relation (12) shows that this control is done by controlling a traction effort $(F_{t1} + F_{t2})$ where each wheel contributes to the advance of the vehicle. However, the inversion of the COG requires the use of a controller where the ergonomic analyzes showed that the driver wishes to keep the control of traction effort by acting on an accelerator pedal in order to control the vehicle speed. In this work, we admit that the action of the driver provides the reference of the total traction effort $(F_{t1} + F_{t2})_{ref}$, Fig. 10. The difficulty of this reference is how to distribute the forces between both wheels (F_{t1-ref} and F_{t2-ref}). The solution of this difficulty can be solved by adding a condition to the inversion of the rigid relation. This condition ($F_{t1-ref} = F_{t2-ref}$) is relating to the stability of the vehicle to imbalance the forces transmitted to each wheel which is closer to the equivalent torques imposed by the classical mechanical differential.

3.1.2 Inversion of the converter CR

We should now define the speed of each wheel in order to ensure the balance of the traction forces. However, the problems which we will face are the nonlinearity and the badly known of the relation to reverse which depends of the road conditions. In the following work, we propose two methods to solve these problems.

3.2. Anti-skid strategy by slip control

The proposed solution will be obtained from the maximum control structure Fig. 9. In this case, the solution to be used to reverse the converter CR is based on the

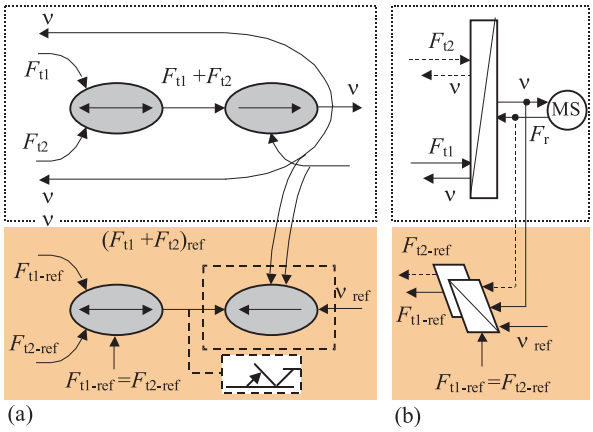

Fig. 10. Modulation of the traction effort: (a) COG and (b) EMR

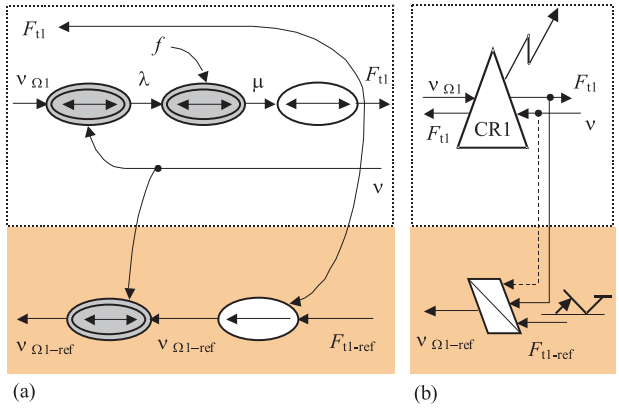

Fig. 12. Inversion of the converter CR: (a) COG; (b) EMR

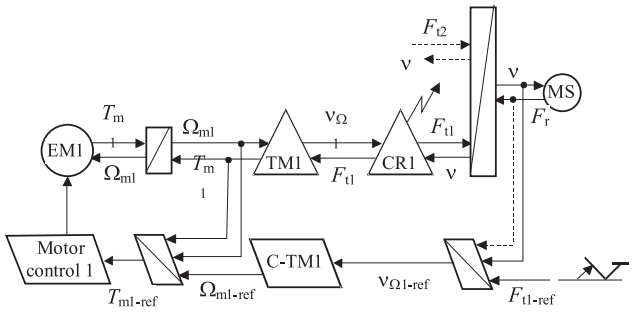

Fig. 11. Control structure deduced from the inversion.

principle of inversion of a badly known rigid relation. We can now apply with this type of relation, the principles of inversion of a causal relation which will minimize the difference between the output and its reference by using a classical controller. The principle of this strategy is based on Fig. 11.

3.2.1 Inversion of relation CR1

Figure 12 shows the COG inversion of relation CR1. We need now the measurements or estimations of the variables speed and traction effort of each wheel. The linear velocity estimation permits a true decoupling in the control of both wheels [20] and the definition of the reference speed which is given by the following equation:

$$V_{\Omega 1\_ref} = \frac{v}{1-\lambda_{1\_ref}}\,. \tag{13}$$

In the control structure, the maximum slip is limited to 10 % which constitutes the real function anti-skidding [21].

The maximum control structure will be used in simulation to validate the global modelling of the system. The EMR and MCS are directly transposed in Matlab-Simulink software, Fig. 12(a).

3.2.2 Simulation results of the MCS control

The same tests are carried out as previously, Fig. 7. We notice from Fig. 13(a) that this type of MCS control permits to avoid the skid phenomenon and both wheel speeds are practically identical. This result is obtained by limiting the slip of wheel 1 to 10 %, Fig. 13(e). An increase of slip beyond that value will not allow to reduce the difference between the traction forces, Fig. 13(g), and the adherence level will not physically permit to transmit the desired traction effort. The force produced by wheel 1 is limited to 950 N. The adapted reduction of torque on wheel 1, Fig. 13(i), however has resulted in good dynamic performance. Figure 13(e) shows the regulation of wheel slip in order to maintain the slip coefficient λ in the adhesive region. We notice that the value is maintained below 10 %.

3.3 Anti-skid strategy by BMC

3.3.1 General analysis of the BMC

The principal objective of this structure of control is to force the output of the process to track the output of the model behaviour , by using an adaptation controller [22–24], Fig. 14. In the four-block representation, the adaptation output acts directly on the process by a supplementary input. The adaptation mechanism can be a simple gain or a classical controller [25].

In this particular case where our process is a nonlinear system, the use of a linear corrector is largely sufficient to obtain all the desired performances in term of stability and precision for any operating point.

3.3.2 Choice of the model

The first step to be made is to establish a behaviour model. In this case, we choose a mechanical model without slip [26], which will be equivalent to the contact wheel-road in the areas known as pseudo-slip [27], Fig. 3(b). This model can be considered as an ideal model. However, the inertia moments of the elements in rotation and the mass of the vehicle can be represented by the total inertia moments J_{t_mod} of each shaft motor which is given by:

$$J_{t\_mod} = \tilde{J}\Omega + \tilde{M}\left(\tilde{k}_{red}\tilde{r}\right)^2\,. \tag{14}$$

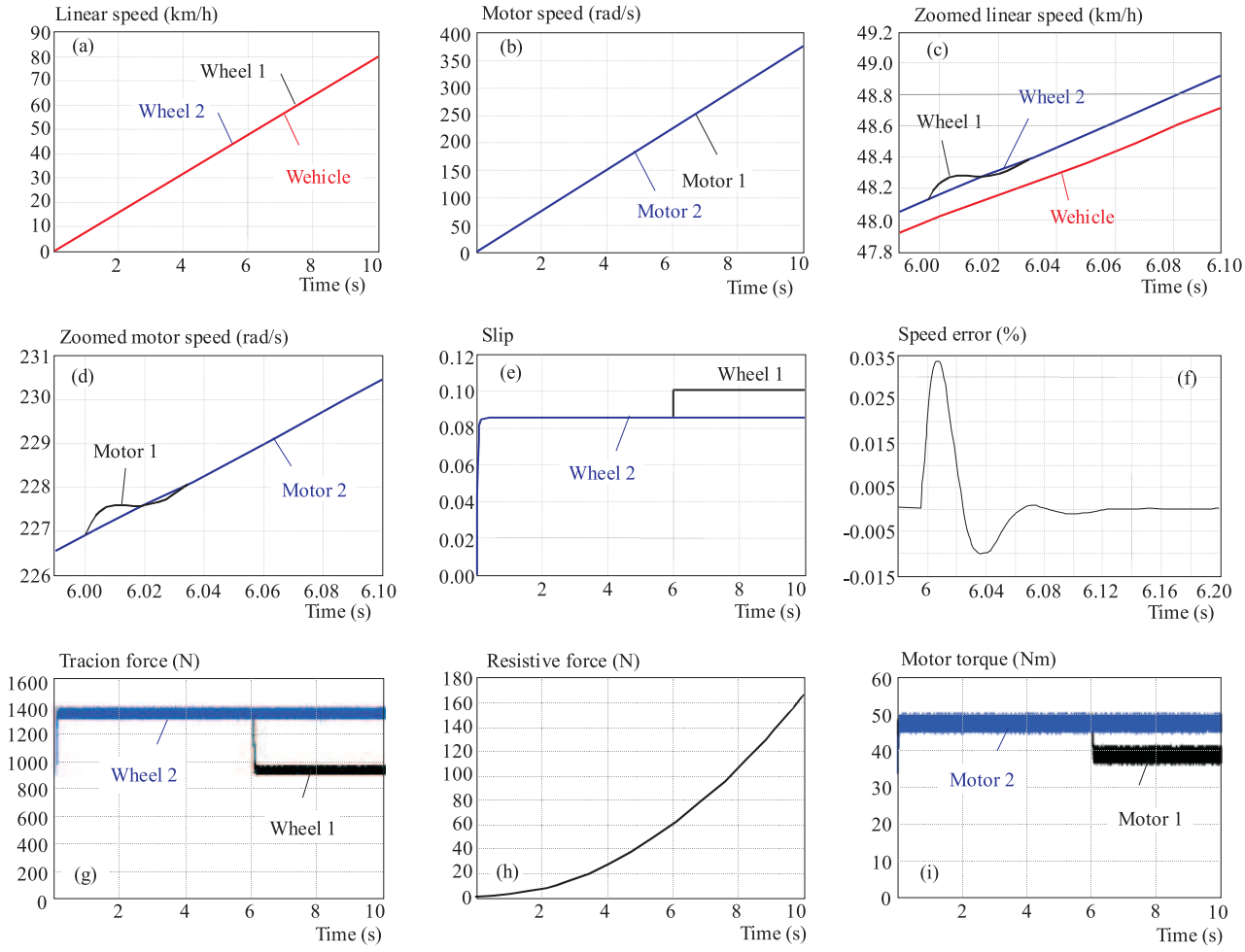

Fig. 13. MCS control-Effect of a loss of adherence

The dynamic equation of the model is given by:

$$J_{t\_mod}\frac{\mathrm{d}\Omega_{mod}}{\mathrm{d}t} = C_{m\_mod} - C_{rm\_mod}\,. \tag{15}$$

By taking into account the wheel slip, the total inertia moments will become:

$$J_t = J_\Omega + M(1-\lambda)(k_{red}r)^2. \tag{16}$$

We now apply the BMC structure for one wheel to solve the skid phenomenon described before. In the Fig. 15, we have as an input the reference torque and as an output the speed of the motor which drives the wheel. However, the main goal of this structure of control is to force the speed Ω_m of the process to track the speed Ω_{m_mod} of the model by using an adaptation controller.

3.3.3 Application of the BMC control to the traction system

It was shown that the state variables of each accumulator are not affected with the same manner by the skid phenomenon. The speed wheel is more sensitive to this phenomenon than that of vehicle, in a homogeneous ratio to the kinetic energies, Fig. 8(a). Hence, the motor speed is taken as the output variable of the model used in the BMC control. The proposed control structure is given by Fig. 16.

From this structure, the input reference is kept as a traction force (F_{t1-ref}) and from the behaviour model without slip, the relation between the motor torque and the traction force is expressed as:

$$F_{t-mod} = \frac{1}{\tilde{m}_{red}\tilde{m}}T_{m-mod}\,. \tag{17}$$

3.3.4 Simulation results of the BMC control

We simulate now the whole system, Fig. A.2, by applying a skid phenomenon at $t = 6$ s to wheel 1 which is driven by motor 1. This skid occurs when moving from a dry road ($\mu_1(\lambda)$) to a slippery road ($\mu_2(\lambda)$) which leads to a loss of adherence, Fig. 7(a). The reference traction force of each wheel is maintained to 1350 N during the acceleration mode.

A first consequence of this BMC strategy is that the speeds of the two motors are equals, Fig. 17(b). The

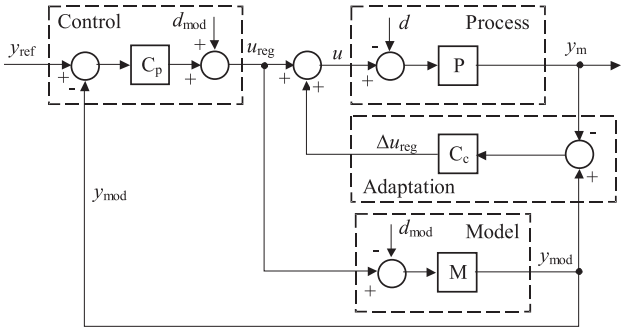

Fig. 14. Behaviour model control structure.

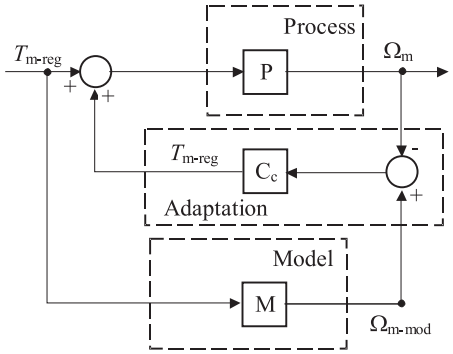

Fig. 15. BMC control applied to one wheel.

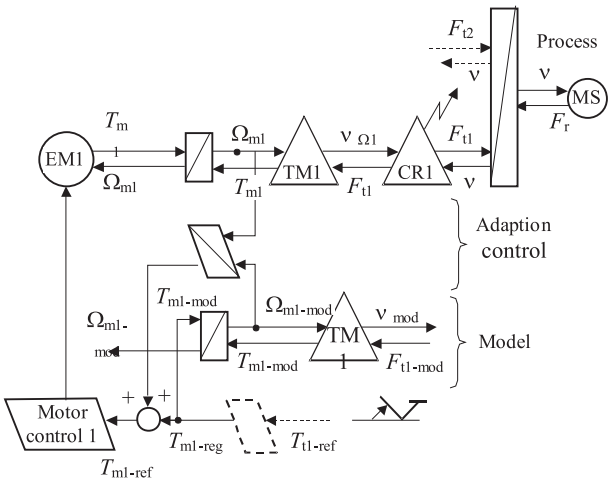

Fig. 16. BMC structure applied to the traction system.

behaviour models being identical and by supposing that the corrector C_c (Proportional-Integral) tends to cancel the difference between the speed of a wheel and its model, we can write:

$$\Omega_{m1\_mod} = \Omega_{m2\_mod} = \Omega_{m1} = \Omega_{m2}\,. \qquad (18)$$

The effect of the loss of adherence results in a strong reduction in the traction force F_{t1} (approximately 20 %) and temporarily an increase of the traction force F_{t2} after $t = 6$ s. The trajectories of the traction forces are illustrated on the Fig. 17(g).

Concerning the speed, we notice that the speed of wheel 1 remains constant and the skid phenomenon has completely disappeared, Fig. 17(a). This good behaviour is obtained due to a reduction of the motor torque 1, Fig. 17(i), which enables the effected wheel to be re-adhered.

The influence of the disturbance on the wheel speeds in both controls is shown in Fig. 18(a). An error is used to compare the transient performances of the MCS and the BMC, Fig. 18(b). This figure shows clearly that the perturbation effect is negligible in the case of BMC control and demonstrates again the robustness of this new control.

4 CONCLUSION

In this paper, new anti-skid control for electric vehicle (EV) is proposed and discussed. This work contributes to the study of the stability of the electric vehicle using the control of the anti-skid systems. We proposed in this work, a new structure of control to solve the mechanical coupling. An optimal structure is obtained based on the formalism suggested by the energetic macroscopic representation. The use of this tool clarifies the anti-skid phenomenon to ensure the stability of the vehicle. The anti-skid control is realized by using two different structures: the maximum control structure and the behaviour model control. However, the simulations carried out showed that the behaviour model control solved the non linear problem of adhesion in which the skid phenomenon has completely disappeared and the stability of vehicle is assured.

Abreviations

COG – Causal Ordering Graph
EC – Electrical Coupling
EM – Electrical machine
EMR – Energetic Macroscopic Representation
ES – Electrical Source
EV – Electric Vehicle
MC – Mechanical Coupling
MCS – Maximum Control Structure
MMS – Multi-machine Multi-converter Systems
MS – Mechanical Source
PMSM – Permanent Magnet synchronous Machine

Appendix

Table 1. The Specifications of the Vehicle Used in Simulation.

Parameter	Symbol	Unit	Value
Vehicle total mass	M	kg	1200
Wheel radius	r	m	0.26
Aerodynamic drag coefficient	C_d	$\mathrm{N/(ms)^2}$	0.25
Vehicle frontal area	S	$\mathrm{m^2}$	1.9
Gearbox ratio	k_{red}	–	1/7.2
Efficiency of the gearbox	η	–	0.98

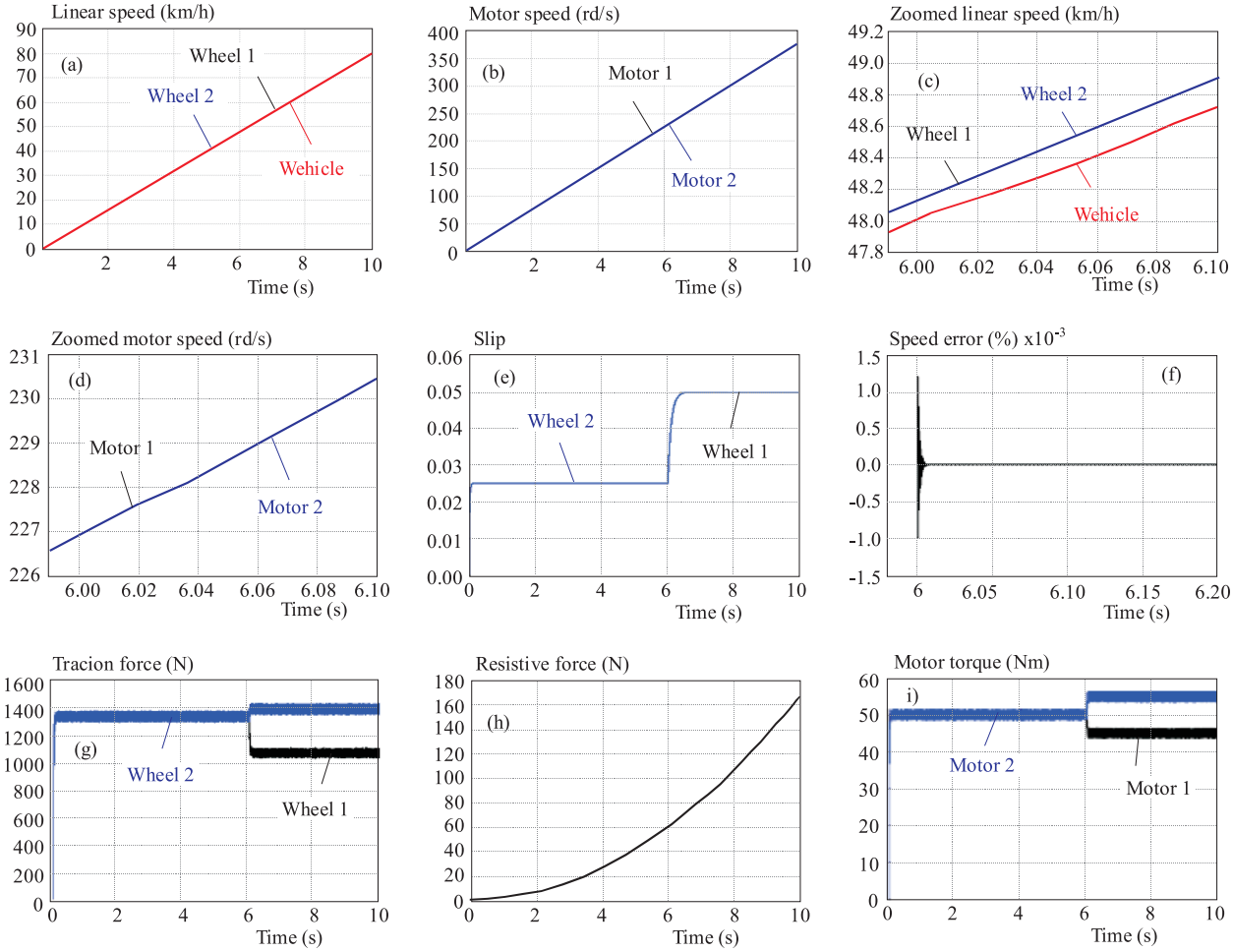

Fig. 17. BMC control-Effect of a loss of adherence.

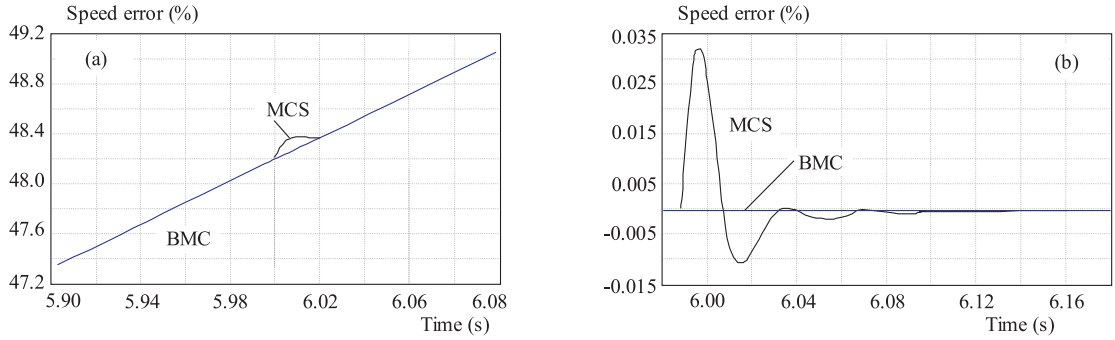

Fig. 18. Effect of a loss of adherence of MCS and BMC controls: (a) Wheel speeds; (b) Speed errors.

Table 2. The specifications of motors.

Parameter	Symbol	Unit	Value
Resistance	R	Ω	0.03
d-axis inductance	L_d	H	2×10^{-4}
q-axis inductance	L_q	H	2×10^{-4}
Permanent magnet flux	Φ_f	Wb	0.08
Pole pairs	p	-	4

References

[1] BOUSCAYROL, A.—DAVAT, B,—DE FORNEL, B.—FRANÇOIS, B.—HAUTIER, J. P.—MEIBODY-TABAR, F.—MONNMASSON, E.—PIETRZAK-DAVID, M.—RAZIK, H.—SEMAIL, E.—BENKHORIS, F. : Control Structures for Multi-Machine Multi-Converter Systems with Upstream Coupling, Mathematics and Computers in Simulation, vol. 63, Elsevier, 2003, pp. 261-270.

[2] BOUSCAYROL, A.—DAVAT, B. DE FORNEL, B.—FRANÇOIS, B.—HAUTIER, J. P.—MEIBODY-TABAR, F.—PIE-

TRZAK-DAVID, M.: Multi-Machine Multi-Converter Systems for Drives: Analysis of Couplings by a Global Modelling, in: Proceedings of the IEEE-IAS Annual Meeting, Rome, October 2000, CD-ROM (common paper of GREEN, L2EP and LEEI, according to the MMS project of GdR-SDSE).

[3] BOUSCAYROL, A.—DAVAT, B.—DE FORNEL, B.—FRANÇOIS, B.—HAUTIER, J. P.—MEIBODY-TABAR, F.: Multi-Machine Multiconverter System: Application for the Electromechanical Conversion, EPJ Appl Phys. **10** (2000), 131-147.

[4] MERCIERA, J. C.—VERHILLE, J. N.—BOUSCYROL, A.: Energetic Macroscopic Representation of a Subway Traction System for a Simulation Model, IEEE-ISIE'04, Ajaccio (France), May 2004.

[5] GUSTAFSSON, F.: Monotiring Tire-Road Friction using the Wheel Slip, IEEE Control Systems Magazines **18** No. 4 (1998), 42–49.

[6] GUSTAFSSON, F.: Slip Based Tire-Road Friction Estimation, Automatica **33** No. 6 (1997), 1087–1099.

[7] HORI, Y.—TOYODA, Y.—TSURUOKA, Y.: Traction Control of Electric Vehicule Based on the Estimation of Road Surface Condition. Basic Experimental Results using the Test EV "UOT Electric March", IEEE. Trans. on Industry Applications **34** No. 5 (1998), 1131–1138.

[8] GUILLAUD, X.—DEGOBERT, P.—HAUTIER, J. P.: Modelling, Control and Causality: the Causal Ordering Graph, 16^{th} IMACS World Congress, CD-ROM, Lausanne, Switzerland; August 2000.

[9] EHSANI, M.—RAHMAN, K. M.—TOLIYAT, H. A.: Propulsion System Design and Hybrid Vehicles, IEEE Transactions on Industrial Electronics **44** No. 1 (1997), 19–27.

[10] MULTON, B.: Motorisation des véhicules électriques. Techniques de l'ingénieur, Article E3996, volume E5, Paris, Février 2001.

[11] WONG, J. Y.: The Theory of Ground Vehicle, WileyInterscience Publication, 1993.

[12] ARNET, B.—JUFER, M.: Torque Control on Electric Vehicles with Separate Wheel Drives, Proceeding of EPE'97, Trondhein, vol. 4, 1997, pp. 39–40.

[13] HARTANI, K.—BOURAHLA, M.—MAZARI, B.: New Driving Wheels Control of Electric Vehicle, Journal of Electrical Engineering **5** (2005), 36–43.

[14] BOURAHLA, M.—HARTANI, K.: Electric Vehicle Speed Control: An Electronic Differential Based System, ICGST International Journal on Automatic Control and System Engineering **5** No. 4 (2005), 59–66.

[15] SADO, H.—SAKAI, S.—HORI, Y.: Road Condition Estimation for Traction Control in Electric Vehicle, In Proc. IEEE Int. Symp. Industrial Electronicq, Solvenia, 1999, 973–978.

[16] OKANO, T.—TAI, C.—INOUE, T.—UCHIDA, T.—SAKAI, S.—HORI, Y.: Vehicle Stability Improvement Based on MFC indepedently Installed on 4 Wheels-Basic Experiments using "UOT Electric March II", In proc. PCC-Osaka, 2002.

[17] SAKAI, S.—HORI, Y.: Advantage of Electric Motor for Antiskid Control of Electric Vehicle, EPE Journal **l.11** No. 4 (2001), 26–32.

[18] ARNET, B.—JUFER, M.: Motor Short-Circuit on Vehicles with Multiple Drives, Proceeding on CD-ROM, EVS 1998, Brussels (Belgiem), September 1998.

[19] BOUSCAYROL, A.—DELARUE, P.: Simplifications of the Maximum Control Structure of a Wind Energy Conversion System with an Induction Generator, Int. J. Renew Energy Eng. **4** No. 2 (2002), 479-485.

[20] PIERQUIN, J.—BOUSCAYROL, A.—HAUTIER, J. P.: Commande optimisée d'un ensemble multimoteur dans une application de traction électrique, JDA'99, Nancy, Actes 1999, 245–248.

[21] PIERQUIN, J.: Commande d'un systeme multimachine asynchrone dans une application de traction électrique. Rapport de collaboration entre L2EP Lille et le LEEI Toulouse dans le cadre du projet SMM du GdR-SDSE, Janvier 2000.

[22] HAUTIER, J. P.—GARON, J. P.: Systemes automatiques, Tome 2, Commande de processus, Edition Ellipses, Paris, 1997.

[23] VULTURESCU, B.—BOUSCAYROL, A.—HAUTIER, J. P.—GUILLAUD, X.—IONESCU, F.: Behaviour Model Control of a DC Machine, ICEM2000, Conference Espoo (Finland). August 2000.

[24] PIERQUIN, J.—ESCANE, P.—BOUSCAYROL, A.—PIETRZAK-DAVID, M.—HAUTIER, J. P.—DE FORNEL, B.: Behaviour Model Control of a High Speed Traction System, EPE-PEMC 2000 Conference, Košice (Slovak Republic), September 2000.

[25] VULTURESCU, B.—BOUSCAYROL, A.—IONESCU, F.—HAUTIER, J. P.: Behaviour Model Control for Cascaded Processes: Application to an Electrical Drive, Computers and Electrical Engineering, vol. 30, Elsevier, 2004, pp. 509–526.

[26] HAUTIER, J. P.—GARON, J. P.: Convertisseurs statiques: méthodologie causale de modélisation et de commande, Edition Technip, Paris, 1999.

[27] LOCHOT, C.: Modélisation et caractérisation des phénomenes couplés dans une chane de traction ferroviaire asynchrone, These de doctorat de l'INP Toulouse, 1999.

Received 18 April 2007

Hartani Kada is born in Saida (Algeria) in 1976. He obtained a diploma of engineer in Electrotechnic in 1997. He received his master at University of Sciences and Technology of Oran (Algeria) from 2001 at 2003. He is an associate professor at university center of Saida. His fields of interest include: multimachines multiconverters systems, Antilock brake system, Traction control system, Anti-skid control for electric vehicle.

Bourahla Mohamed is born in Naama, Algeria, in 1952. He received the Doctorate degree (Aspirantus) in Electrical Drives from the Technical University of Budapest, Hungaria and "Doctorat d'Etat" degree in Power Electronics from the University of Sciences and Technology of Oran (USTO), Algeria in 1983 and 1995, respectively. From 1983 to 1987 he teaches and conducts research in the area of Power Electronics and Electrical Drives at the Institute of Electrotechnics of USTO. From 1987 to 1991 he was a researcher at the University of Technical Sciences of Montpellier, France, where he conducts research work on GTO thyristor for electrical traction application. He is currently an associate Professor where he continues to conduct research in Power Semi Conductor Devices, Powers Electronics Structures (PES) in applications of Electrical traction, solar energy, Telecommunication and Medical.

Yahia Miloud was born in June 1955. He received the BEng degree from Bradford University, UK in 1980, the MSc degree from Aston University in Birmingham, UK in 1981 and the PhD degree from Electrical Machines Department of Electrical and Electronic engineering, University of Oran (UST0), Algeria in 2006. From 1982 to 1988 he was a senior Engineer for Sonatrach LNG1 plant, Arzew Algeria where he was in charge of the method section of the maintenance department and responsible for the operation of all UPS of the plant . In 1988 he joined the department of Electrotechnics at the university center of Saida, Algeria where he is still working as a lecturer. His main area of research includes power electronics, multilevel inverters, and intelligent control of ac drives. His current activities include direct torque control, fuzzy control of ac drives and electrical vehicles.